

Measurement of thoron gas in the environment using a Lucas scintillation cell

This article has been downloaded from IOPscience. Please scroll down to see the full text article.

2010 J. Radiol. Prot. 30 597

(<http://iopscience.iop.org/0952-4746/30/3/013>)

View [the table of contents for this issue](#), or go to the [journal homepage](#) for more

Download details:

IP Address: 222.29.111.66

The article was downloaded on 05/09/2012 at 12:34

Please note that [terms and conditions apply](#).

Measurement of thoron gas in the environment using a Lucas scintillation cell

Lei Zhang¹, Jian Wu¹, Qiuju Guo^{1,3} and Weihai Zhuo²

¹ State Key Laboratory of Nuclear Physics and Technology, School of Physics, Peking University, Beijing 100871, People's Republic of China

² Institute of Radiation Medicine, Fudan University, Shanghai 200032, People's Republic of China

E-mail: qjguo@pku.edu.cn

Received 19 January 2010, in final form 17 May 2010, accepted for publication 25 May 2010

Published 8 September 2010

Online at stacks.iop.org/JRP/30/597

Abstract

A simple and fast method for measuring the concentration of ^{220}Rn in the environment was developed based on the AB-5 portable radon measuring device. First, background counts were measured with a Lucas scintillation cell (LSC), then air sampling measurement was started immediately and lasted for 1 min; the ^{220}Rn concentration could be calculated from the counts before and after sampling as well as the theoretical detection efficiency. Results of theoretical calculations showed that in a pure ^{220}Rn environment the lower detection limit of the LSC would be some 65 Bq m^{-3} (with a confidence level of 70%). The experimental results showed that compared with a RAD7 monitor in pure ^{220}Rn or mixed $^{222}\text{Rn}/^{220}\text{Rn}$ environments the deviations were less than $\pm 10\%$. This method can also be used for quantitative measurement of ^{220}Rn concentration.

(Some figures in this article are in colour only in the electronic version)

1. Introduction

Radon (^{222}Rn) and thoron (^{220}Rn) gases are isotopes produced from the ^{238}U and ^{232}Th decay chains, respectively; they exist naturally in the environment. They decay into some short-lived progeny which can be inhaled into the respiratory organs and cause internal radiation exposure.

Radon and its progeny have been widely studied since 1960s due to its significant contributions to radiation exposure of the public. In contrast to this, there had been limited studies and few representative data for thoron until Schery (1990) and Steinhäusler (Steinhäusler *et al* 1994, Steinhäusler 1996) proposed the importance of thoron exposure. The main reason for this situation was that the levels of thoron and its progeny were considered

³ Author to whom any correspondence should be addressed.

to be very low due to the short half-life of thoron (55.6 s), and it was thought that the dose contribution to the public from thoron and its progeny could be ignored compared with that from radon and its progeny.

However, some high thoron concentrations have been reported in recent years in Asia (Doi and Kobayashi 1994, Guo *et al* 2000, Shang 2008), and the potential high risk of exposure to indoor thoron and its progeny were indicated. During the last decade some new methods and devices were developed and some representative data collected for thoron concentration measurement (Yamada *et al* 2005, Zhuo *et al* 2002, Guo *et al* 1995).

To understand the spatial distribution of thoron concentration, measurements of thoron gas are necessary, even though direct measurement of thoron progeny is much more important for dose evaluation. However, it is difficult to measure thoron concentration accurately because of its rather short half-life, and calibration of thoron detectors has not yet been perfected in most laboratories. In a radon/thoron mixed environment, the problems caused by mutual interference between radon and thoron have still not been completely resolved. Although some commercial radon monitors such as RAD7 (DurrIDGE, USA) and RTM2100 (Sarad, Germany) that use an electrostatic collection technique and alpha-spectrum analysis can measure radon and thoron concentration simultaneously, most such instruments have problems with the status of desiccant or the humidity of the external environment.

The Lucas scintillation cell (LSC) is a classic scintillation detector which is based on the principle of counting of photons resulting from the interaction of alpha particles produced by radon/thoron and their progeny with the ZnS(Ag) scintillator. Falk (Falk *et al* 1992) first realised the measurement of thoron gas at an environment level using a LSC and multiple time analysis by analysing the pulse event of ^{216}Po . This method can detect very low thoron concentrations ($\sim 1 \text{ Bq m}^{-3}$) but uses expensive multiple time analysis which not suitable for other laboratories. The AB-5 portable radiation detector produced by Pylon Electronics (Canada) coordinates with the LSC for radon concentration measurement. Since the device principle is clear and operation is simple, it is suitable for use in the environment. Previous researchers (Hutter 1995, Tokonami *et al* 2002, Eappen *et al* 2008) have developed many methods using the LSC and AB-5 to measure thoron concentration by selecting different counting times and different sampling methods; some detection efficiencies of radon/thoron gas and daughters were also calculated using MC (Monte Carlo) methods. But all the methods have one problem or another; they either may or may not consider the energy threshold of ZnS(Ag), given the detection limits, and the counting time required more optimisation for field measurement.

For accurate measurement of thoron concentration we studied and developed a method using the LSC and AB-5; comparative experiments were carried out in both pure thoron and mixed radon/thoron. We discuss the detection efficiencies and detection limits in detail.

2. Materials and methods

2.1. The Lucas scintillation cell

Two kinds of LSC, models 110A and 300A, were involved in this study. The 110A cell is a cylindrical vessel, 53 mm in diameter and 70 mm high, with an inner volume and active area of $1.51 \times 10^{-4} \text{ m}^3$ and $1.88 \times 10^{-2} \text{ m}^2$, respectively. The 300A cell is 53 mm in diameter and 124 mm high, with an inner volume and active area of $2.70 \times 10^{-3} \text{ m}^3$ and $2.77 \times 10^{-2} \text{ m}^2$, respectively. All the LSCs have two Swagelok quick connectors on one side of the cylindrical vessel; the other side is a glass window, from where the photons excited by alpha particles are sent to the AB-5 recorder. Figure 1 shows a schematic diagram of the 300A LSC.

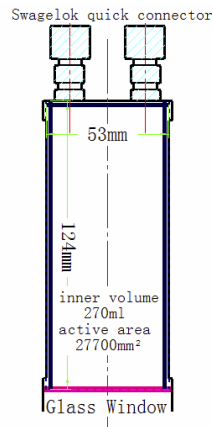


Figure 1. Schematic diagram of a 300A LSC.

The LSC has two sampling modes: grab mode and flow rate mode. For grab mode, a vacuum pump is used to create a vacuum in the LSC, then the through valve is closed and opened at the measurement site. For the flow rate mode the pump inside the AB-5 was used; two quick connectors were connected to the LSC, one to the pump input and one to the sampling site. In our study, only grab mode was used with a 300A LSC.

2.2. Measurement of thoron concentration in pure thoron conditions

In pure thoron conditions without interference of radon, the counting rate of alpha particles simply follows the law of ^{220}Rn decay in the few minutes after sampling, because ^{212}Pb has a much longer half-life than that ^{220}Rn , while the lifetime of ^{216}Po is much shorter than that of ^{220}Rn . Using N'_0 for the background counting rate of the LSC, N'_1 for the counting rate after sampling (here we have chosen the minute after sampling), then the ^{220}Rn concentration is calculated as follows:

$$C_{\text{Tn}} = \frac{N'_1 - N'_0}{S_{\text{Tns}}} k_{\text{Tn}} \quad (1)$$

where S_{Tns} is the calibration factor of equilibrium $^{220}\text{Rn}/^{216}\text{Po}$ ($\text{cpm} (\text{Bq m}^{-3})^{-1}$), k_{Tn} is the correction factor in the counting time T ($=1$ min) caused by the decay of ^{220}Rn , which can be expressed as:

$$k_{\text{Tn}} = \left(\frac{1}{T} \int_0^T \exp(-\lambda_{\text{Tn}} t) dt \right)^{-1} \quad (2)$$

where λ_{Tn} is the decay constant of ^{220}Rn .

2.3. Measurement of thoron concentration in mixed radon/thoron conditions

In mixed radon/thoron conditions the different alpha particle counting rates depend on the half-lives of $^{222}\text{Rn}/^{220}\text{Rn}$, the half-lives of their progeny and the components of $^{222}\text{Rn}/^{220}\text{Rn}$. So at least two time periods were required for counting the rates. As the half-lives of ^{220}Rn and ^{216}Po are quite short, the first counting period was chosen at 0–1 min after sampling. The half-life of ^{212}Pb is much longer than that of ^{222}Rn and its progeny, so the second counting period was chosen at 180–200 min after sampling, when ^{222}Rn and its progeny equilibrating. In general,

thoron concentration is seldom ten times higher than radon concentration, so the alpha particles emitted from $^{212}\text{Po}/^{212}\text{Bi}$ in the second counting period could be ignored.

Taking N'_1 for the first period counting rate and N'_2 for the second period counting rate after sampling, then the ^{222}Rn concentration is calculated as follows:

$$C_{\text{Rn}} = \frac{N'_2 - N'_0 k_{\text{RnM}}}{S_{\text{Rns}} k_{\text{RnW}}} \quad (3)$$

where S_{Rns} is the calibration factor of equilibrium ^{222}Rn and its progeny ($\text{cpm} (\text{Bq m}^{-3})^{-1}$), k_{RnM} is the correction factor in the second counting period T_{M} ($=20$ min) caused by the decay of ^{222}Rn , which can be expressed as:

$$k_{\text{RnM}} = \left(\frac{1}{T_{\text{M}}} \int_0^{T_{\text{M}}} \exp(-\lambda_{\text{Rn}} t) dt \right)^{-1} \quad (4)$$

where λ_{Rn} is the decay constant of ^{222}Rn , and k_{RnW} is the correction factor in the waiting time T_{W} ($=180$ min) before the second counting period due to the decay of ^{222}Rn , which can be expressed as:

$$k_{\text{RnW}} = \exp(-\lambda_{\text{Rn}} T_{\text{W}}). \quad (5)$$

When calculating the ^{220}Rn concentration, it is necessary to deduct the alpha particles emitted from ^{222}Rn and ^{218}Po in the first counting period. Then the ^{220}Rn concentration is calculated as follows:

$$C_{\text{Tn}} = \frac{N'_2 - n_{\text{Rn}} - n_{\text{Po-218}} - N'_1 k_{\text{Tn}}}{S_{\text{Tns}}} \quad (6)$$

where n_{Rn} and $n_{\text{Po-218}}$ respectively represent the average counting rate due to the decay of ^{222}Rn and ^{218}Po ; those can be expressed as:

$$n_{\text{Rn}} = S_{\text{Rn}} \frac{1}{T'} \int_0^{T'} C_{\text{Rn}} \exp(-\lambda_{\text{Rn}} t) dt \quad (7)$$

$$n_{\text{Po-218}} = S_{\text{Po-218}} \frac{1}{T'} \int_0^{T'} C_{\text{Rn}} \frac{\lambda_{\text{Po-218}}}{\lambda_{\text{Po-218}} - \lambda_{\text{Rn}}} [\exp(-\lambda_{\text{Rn}} t) - \exp(-\lambda_{\text{Po-218}} t)] dt \quad (8)$$

where S_{Rn} and $S_{\text{Po-218}}$ are the calibration factors of ^{222}Rn and ^{218}Po ($\text{cpm} (\text{Bq m}^{-3})^{-1}$).

We measure the background count for 10 min before sampling, then count for 1 min immediately after sampling; wait for 180 min and count for 20 min: N_0 , N_1 and N_2 stand for the total background count, the first counting period and the second counting period. Then the radon and thoron concentrations in a radon/thoron mixture can simply be expressed as:

$$C_{\text{Rn}} = 1.024 \frac{N_2/20 - N_0/10}{S_{\text{Rns}}} \quad (9)$$

$$C_{\text{Tn}} = 1.4214 \frac{N_1 - C_{\text{Rn}}(S_{\text{Rn}} + 0.1947 S_{\text{Po-218}}) - N_0/10}{S_{\text{Tns}}} \quad (10)$$

where S_{Rns} , S_{Tns} , S_{Rn} and $S_{\text{Po-218}}$ are the calibration factors of equilibrium ^{222}Rn and its progeny, equilibrium $^{220}\text{Rn}/^{216}\text{Po}$, ^{222}Rn and ^{218}Po ($\text{cpm} (\text{Bq m}^{-3})^{-1}$).

2.4. Detection efficiency and calibration factor

The calibration factor of the LSC is proportional to the detection efficiency. Usually, the instrument was calibrated only in pure ^{222}Rn leaving out the ^{220}Rn calibration facility. So we calculated the detection efficiencies of $^{222}\text{Rn}/^{220}\text{Rn}$ and their progeny through Monte Carlo

Table 1. The detection efficiencies of $^{222}\text{Rn}/^{220}\text{Rn}$ and their progeny in 110A and 300A LSCs.

Nuclide	State	The detection efficiency in 110A (%)	The detection efficiency in 300A (%)
^{222}Rn	Evenly distributed in LSC	69.17 ± 0.18	68.37 ± 0.16
^{218}Po	Evenly distributed in LSC	76.01 ± 0.06	75.81 ± 0.10
$^{218}\text{Po}'$	Evenly distributed on wall	72.84 ± 0.13	73.11 ± 0.15
^{214}Po	Evenly distributed on wall	84.53 ± 0.12	86.68 ± 0.07
^{220}Rn	Evenly distributed in LSC	79.22 ± 0.12	79.42 ± 0.18
^{216}Po	Evenly distributed in LSC	83.32 ± 0.11	84.30 ± 0.11

Table 2. The calibration factor of $^{222}\text{Rn}/^{220}\text{Rn}$ and their progeny in a 300A LSC.

	Description	Calibration factor (cpm (Bq m ⁻³) ⁻¹)
S_{Rns}	Equilibrium ^{222}Rn and its progeny	0.0370
S_{Tns}	Equilibrium ^{220}Rn and ^{216}Po	0.0265
S_{Rn}	^{222}Rn	0.0111
$S_{\text{Po-218}}$	^{218}Po	0.0123

simulation, and obtained the calibration factor for ^{220}Rn by comparison of the simulated detection efficiency and experimental detection efficiency of ^{222}Rn .

The following assumptions were used when simulating the detection efficiency of $^{222}\text{Rn}/^{220}\text{Rn}$ and their progeny:

- (1) ^{222}Rn and ^{220}Rn is evenly distributed in the LSC;
- (2) ^{216}Po has the same distribution, as its half-life is so short;
- (3) ^{218}Po has a probability of attaching to the wall of the LSC as its half-life is neither too short nor too long;
- (4) ^{214}Po is evenly distributed on the wall of LSC as it has enough time to attach to the wall.

Taking into account the energy threshold of ZnS(Ag), MC calculation results for the detection efficiency of every nuclide in 110A and 300A LSCs are shown in table 1 (with the number of target particles ten times $\times 10^5$ /time). These results are quite close to the results given in a previous paper (Tokonami *et al* 2002), but show some differences, mainly because we considered the energy threshold of ZnS(Ag) and the possible distribution of ^{218}Po .

When calibrating in pure ^{222}Rn , the LSC records the alpha particles emitted from ^{222}Rn , ^{218}Po and ^{214}Po which are in equilibrium. The average detection efficiency of ^{222}Rn and its progeny E_{Rns} can be expressed as:

$$E_{\text{Rns}} = \frac{1}{3}(E_{^{222}\text{Rn}} + xE_{^{218}\text{Po}} + E_{^{218}\text{Po}'} + E_{^{214}\text{Po}}) \approx 0.7606 + 0.009x \quad x \in [0, 1] \quad (11)$$

where x is the probability of ^{218}Po not being attached to the wall of the LSC. As the calibration result from the factory gives an average detection efficiency of 0.76, so all ^{218}Po are attached to the wall. At the same time, the average detection efficiency of ^{220}Rn and ^{216}Po E_{Tns} is 0.8186.

The calibration factor is equal to the average detection efficiency multiplied by the number of alpha particles emitted from $^{222}\text{Rn}/^{220}\text{Rn}$ and their progeny in unit activity. The calibration factors of $^{222}\text{Rn}/^{220}\text{Rn}$ and their progeny in a 300A LSC are shown in table 2.

Using the calibration factor, the simplified formula for the ^{220}Rn concentration in pure ^{220}Rn and mixed $^{222}\text{Rn}/^{220}\text{Rn}$ can be expressed as:

$$\text{In pure } ^{220}\text{Rn} \text{ condition:} \quad C_{\text{Tn}} = 53.585(N_1' - N_0'). \quad (12)$$

$$\text{In mixed } ^{222}\text{Rn}/^{220}\text{Rn} \text{ condition:} \quad C_{\text{Tn}} = 53.585(N_1' - 0.0135C_{\text{Rn}} - N_0'). \quad (13)$$

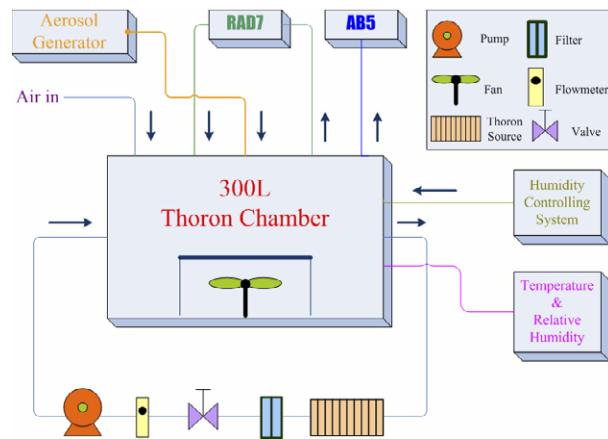


Figure 2. Sketch map of the thoron chamber at Peking University.

Table 3. The lower detection limit of ^{220}Rn concentration using this method (Bq m^{-3}).

Confidence interval	Pure ^{220}Rn	Mixed $^{222}\text{Rn}/^{220}\text{Rn}$		
		$^{222}\text{Rn} = 50 \text{ Bq m}^{-3}$	$^{222}\text{Rn} = 200 \text{ Bq m}^{-3}$	$^{222}\text{Rn} = 1000 \text{ Bq m}^{-3}$
70%	64.3	96.2	153	308
95%	303	404	584	1074

2.5. Lower detection limit

Assuming that the type I and type II errors are the same, the lower detection limits could be (Huang 2004):

$$L_D = K^2 + 2K\sqrt{2M_B} \quad (14)$$

where K is the probability of error and M_B is the expected background. In pure ^{220}Rn , M_B is the background count rate of the LSC ($=0.4 \text{ cpm}$); in mixed $^{222}\text{Rn}/^{220}\text{Rn}$, the M_B of ^{220}Rn is the sum of the the background count rate of the LSC and the counting rate of ^{218}Po , that is $M_B = 0.0135C_{\text{Rn}} + \text{BG}$. The lower detection limits of ^{220}Rn concentration under different confidence intervals (70% and 95%) in pure ^{220}Rn and mixed $^{222}\text{Rn}/^{220}\text{Rn}$ conditions are shown in table 3.

2.6. Intercomparison experiments

To confirm the validity of this method, a series of intercomparison experiments were carried out in our home-made thoron chamber with different levels of ^{220}Rn and mixed $^{222}\text{Rn}/^{220}\text{Rn}$ concentrations. A sketch map of the thoron chamber at Peking University is shown in figure 2.

The thoron chamber in Peking University is a cubic watertight chest made with anti-static organic glass; it has an inner volume of 300 l with a built-in fan to evenly distribute ^{220}Rn . The ^{220}Rn source was provided by lantern mantles (content activity ^{232}Th : $131 \pm 4 \text{ kBq kg}^{-1}$, ^{238}U : $61 \pm 20 \text{ Bq kg}^{-1}$, no ^{226}Ra found) (Sorimachi 2009) outside the chamber, and the thoron concentration was controlled by adjusting the flow rate and the number of lantern mantles. A humidity controlling system and air-conditioner in the room kept the temperature and humidity stable.

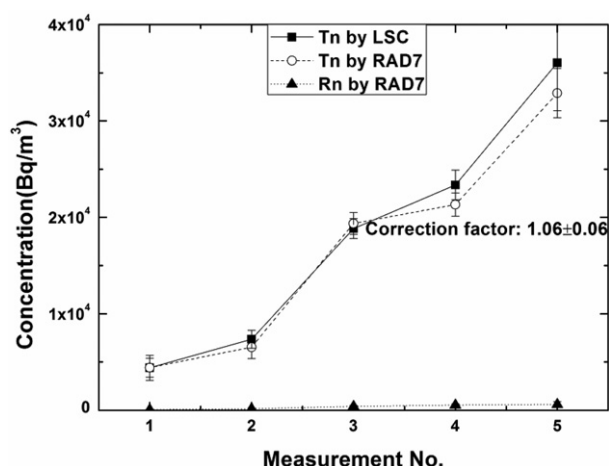


Figure 3. Comparison of the results of the LSC and RAD7 in pure ^{220}Rn .

Two kinds of intercomparison experiment were finished separately under pure ^{220}Rn and mixed $^{222}\text{Rn}/^{220}\text{Rn}$. The comparison device is a RAD7 (DurrIDGE Co., USA) which had been calibrated at the thoron chamber (the reference standard of China) in Hengyang, Hunan Province (Yang 2006). ^{222}Rn is generated from a liquid radium source and pumped into the thoron chamber to obtain mixed $^{222}\text{Rn}/^{220}\text{Rn}$.

3. Results and discussion

3.1. Intercomparison experiment in pure ^{220}Rn

A comparison of the results for the LSC and RAD7 in pure ^{220}Rn is shown in figure 3.

The measurement results given by the LSC are a little higher than those from the RAD7 in most concentrations. The average deviation of the two devices is 6%, with all the deviations <15%, and the deviation have no obviously correlation with the ^{220}Rn concentration. At the same time, we found that the ^{222}Rn concentration were not zero even in pure ^{220}Rn , and the ^{222}Rn concentration increased with the ^{220}Rn concentration, which might be a problem with the analysing spectrum in this instrument itself.

3.2. Intercomparison experiment in mixed $^{222}\text{Rn}/^{220}\text{Rn}$

A comparison of the results of the LSC and RAD7 in mixed $^{222}\text{Rn}/^{220}\text{Rn}$ is shown in figure 4.

All the intercomparison experiments were completed under conditions where the ^{220}Rn concentrations are higher than the ^{222}Rn concentrations. All the ^{220}Rn concentrations show no significant difference between LSC and RAD7, and deviations are within $\pm 10\%$. But the ^{222}Rn concentrations of the LSC are lower than the result of the RAD7, and the deviations increase with the ^{220}Rn concentration. The reason might be the problem that RAD7 cannot properly distinguish the alpha particles emitted from ^{212}Bi and ^{218}Po as ^{212}Bi accumulates in RAD7 with continuous measurement, resulting in the higher ^{222}Rn concentration given by the RAD7.

When the ^{220}Rn concentration is lower than the ^{222}Rn concentration, the alpha particles emitted from ^{218}Po may make a large contribution to the counting rate in the first counting period, which may cause the measured ^{220}Rn concentration to show a large deviation.

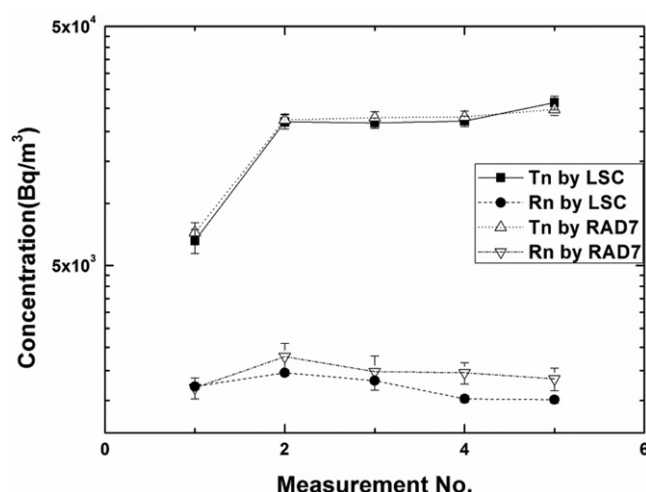


Figure 4. Comparison of the results of the LSC and RAD7 in mixed $^{222}\text{Rn}/^{220}\text{Rn}$.

4. Conclusion

In order to study the possibility of accurate measurement of thoron concentration using a LSC, a simple and fast method for measuring the environmental concentration of ^{220}Rn was developed based on the AB-5 portable radon measuring device. Theoretical calculation results show that in pure ^{220}Rn the lower detection limit is up to about 65 Bq m^{-3} (confidence level 70%). Though the lower detection limit changed with the ^{222}Rn concentration in a mixed $^{222}\text{Rn}/^{220}\text{Rn}$ environment, it can be reduced by accurate measurement of the ^{222}Rn concentration. Compared with the experimental results in pure ^{220}Rn or a mixed $^{222}\text{Rn}/^{220}\text{Rn}$ environment, the deviations with RAD7 were less than $\pm 10\%$. This method using a LSC has the advantages of simple, swift and easy operation, suitable for a reference standard for ^{220}Rn concentration measurement in pure ^{220}Rn environment. This method does not have the uncertainty of spectroscopic analysis and can also be used in environments with a high ^{220}Rn concentration.

References

- Doi M and Kobayashi S 1994 Characterization of Japanese wooden houses with enhanced radon and thoron concentration *Health Phys.* **66** 274–82
- Eappen K P, Nair R N and Mayya Y S 2008 Simultaneous measurement of radon and thoron using Lucas scintillation cell *Radiat. Meas.* **43** 91–7
- Falk R, More H and Nyblom L 1992 Measurements of ^{220}Rn in air using a flow-through Lucas cell and multiple time analysis of recorded pulse events *Radiat. Prot. Dosim.* **45** 111–3
- Guo Q, Sun J and Zhuo W 2000 Potential of high thoron exposure in China *J. Nucl. Sci. Technol.* **37** 716–9
- Guo Q *et al* 1995 Measurements of thoron concentration by passive cup method and its application to dose measurement *J. Nucl. Sci. Technol.* **32** 794–807
- Huang N 2004 Concept and calculation of detection limit in low level radioactive sample measurement *Radiat. Prot. Bull.* **24** 25–32 (in Chinese)
- Hutter A R 1995 A method for determining soil gas thoron concentrations *Health Phys.* **68** 835–7
- Schery S D 1990 Thoron in the environment *J. Air Waste Manage. Assoc.* **40** 493–7
- Shang B 2008 Radon survey in dwellings of Gansu, China: the influence of thoron and an attempt for correction *Radiat. Environ. Biophys.* **47** 367–73
- Sorimachi A 2009 Generation and control of thoron emanated from lantern mantles *Rev. Sci. Instrum.* **80** 015104
- Steinhäusler F 1996 Environmental ^{220}Rn : a review *Environ. Int.* **22** (Suppl. 1) S1111–23

- Steinhäusler F, Hofmann W and Lettner H 1994 Thoron exposure of man: a negligible issue? *Radiat. Prot. Dosim.* **56** 127–31
- Tokonami S *et al* 2002 Simple, discriminative measurement technique for radon and thoron concentrations with a single scintillation cell *Rev. Sci. Instrum.* **73** 69–72
- Yamada Y *et al* 2005 Rn–Tn discriminative measurements and their dose estimates in Chinese loess plateau *Int. Congr. Ser.* **1276** 76–81
- Yang M L 2006 Nanhua thoron chamber-building, uniformity and stability *Proc. China–Japan–Korea Scientists Workshop on Environmental Radon and Thoron Study (Shanghai, March)*
- Zhuo W *et al* 2002 A simple passive monitor for integrating measurements of indoor thoron concentrations *Rev. Sci. Instrum.* **73** 2877–81